Journal of Alloys and Compounds 519 (2012) 161–166

Contents lists available at SciVerse ScienceDirect

Journal of Alloys and Compounds

journal homepage: www.elsevier.com/locate/jallcom

Effects of the mechanical activation of zinc carbonate hydroxide on the formation and properties of zinc oxides

Yanko Dimitriev[a], Maria Gancheva[b,*], Reni Iordanova[b]

[a] University of Chemical Technology and Metallurgy, 1756 Sofia, Bulgaria
[b] Institute of General and Inorganic Chemistry, Bulgarian Academy of Sciences, 1113, Sofia, Bulgaria

ARTICLE INFO

Article history:
Received 13 September 2011
Received in revised form
21 December 2011
Accepted 31 December 2011
Available online 10 January 2012

Keywords:
Mechanochemical synthesis
ZnO
Optical properties
Photocatalytic activity

ABSTRACT

The nanocrystalline ZnO powders were obtained by mechanochemical treatment of zinc carbonate hydroxide. The mechanical activation was carried out in a planetary ball mill (Fritsch–Premium line–Pulversette No 7) by varying of the milling speed. The phase and structural transformation was investigated by X-ray diffraction (XRD) and infrared spectroscopy (IR). The morphology of the obtained ZnO powders was characterized by scanning electron microscopy (SEM). The crystallite size of the samples calculated from XRD and the SEM observation were in the range from 8 to 50 nm. The optical properties were investigated by UV–vis spectroscopy. The photocatalytic activity was studied with respect to the photodegradation of Malachite green (MG) under UV-light irradiation. The milling speed of 500 rpm led to full amorphization of the initial zinc carbonate hydroxide. After heat-treatment at 400 °C of X-ray amorphous sample single ZnO powder (20 nm) was obtained. The direct synthesis of ZnO nanoparticles (8 nm) was achieved at milling speed of 1000 rpm for short time (90 min). The mechanochemically synthesized ZnO powders possess good optical and photocatalytic properties. The additional heat-treatment improved the photocatalytic activity and the transparency of ZnO powders in the visible spectral range.

1. Introduction

ZnO is one of the most important inorganic materials which finds many industrial applications: varistors [1,2], UV-light emitting diodes [3], UV laser [4], gas sensors [5], photocatalysts [6,7] and photovoltaic devices [8]. The properties of ZnO are due to the fact that it is a semiconductor, with a wide band gap of 3.37 eV, large exciton binding energy of 60 meV, chemical and thermal stability [9–11]. The method of preparation as well as crystalline size and morphology of the particles influence the properties of the final product [12–31]. Several methods for the synthesis of ZnO nanoparticles have been reported in the literature: hydrothermal synthesis [13], acid-assisted annealing process [14], co-precipitation [15,16], via H_2O_2 pre-oxidation [17,18], sol gel [19–21], thermal decomposition of zinc carbonate hydroxide [22–25] and mechanochemical synthesis [26–31]. It is well known that the mechanochemical activation generates various types of defects in the structure of materials which lead to a higher reactivity and a reduction of the time needed for the solid state synthesis [32–35]. The future development on this method called "soft mechanochemical method" was suggested by Senna and co-workers using hydroxides, hydrates or carbonates as precursors [34,35]. Thus the processes of chemical reaction can be accelerated. For the first time Tsuzuki and McCormick [26] realized a solid-state displacement reaction between $ZnCl_2$ and Na_2CO_3 by mechanochemical processing, forming of $ZnCO_3$ in a NaCl matrix. The additional heat treatment was used in order to decompose $ZnCO_3$ and to obtain ZnO nanoparticles. This approach was applied latter by other authors [27–31]. The ZnO powders synthesized by this method possess high optical transparency [29,31].

The purpose of this study is to perform soft mechanochemical synthesis of ZnO powders using zinc carbonate hydroxide as a precursor. The advantage of this approach is to avoid the formation of intermediate $ZnCO_3$ and additional heat-treatment for its decomposition. The photocatalytic activity and optical properties of the final products were investigated.

2. Experimental

The zinc carbonate hydroxide (Fluka) which is a mixture of hydrozincite $Zn_5(CO_3)_2(OH)_6$ (JCPDS-14-0256) and $Zn_4(CO_3)_2(OH)_6{\cdot}H_2O$ (JCPDS-03-0787) was subjected to intense mechanical treatment in air using a planetary ball mill (Fritsch–Premium line–Pulversette No 7). Both vials and balls were of stainless steel. Different factors affect the milling process such as: type of mill, milling speed, time, ball-to-powder mass ratio, starting materials, etc. In this investigation we selected two milling speed (500 and 1000 rpm) in order to check their influence on phase and structural transformation during the mechanical activation. The ball-to-powder mass ration and the ball diameter were constant. The samples A and B were mechanically treated as follows:

* Corresponding author. Tel.: +359 2 979 35 88; fax: +359 2 870 50 24.
E-mail address: mancheva@svr.igic.bas.bg (M. Gancheva).

0925-8388/$ – see front matter © 2012 Elsevier B.V. All rights reserved.
doi:10.1016/j.jallcom.2011.12.169

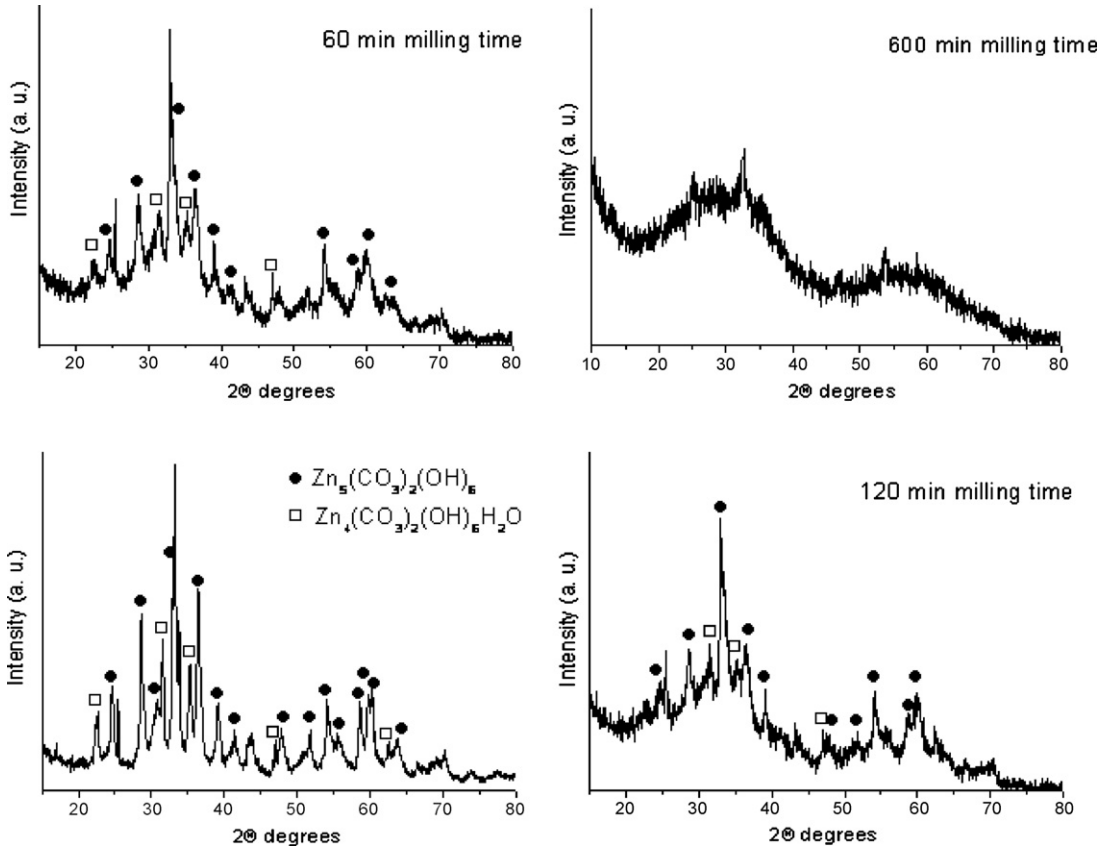

Fig. 1. XRD patterns of the sample A (mechanically treated at 500 rpm) as a function of milling time.

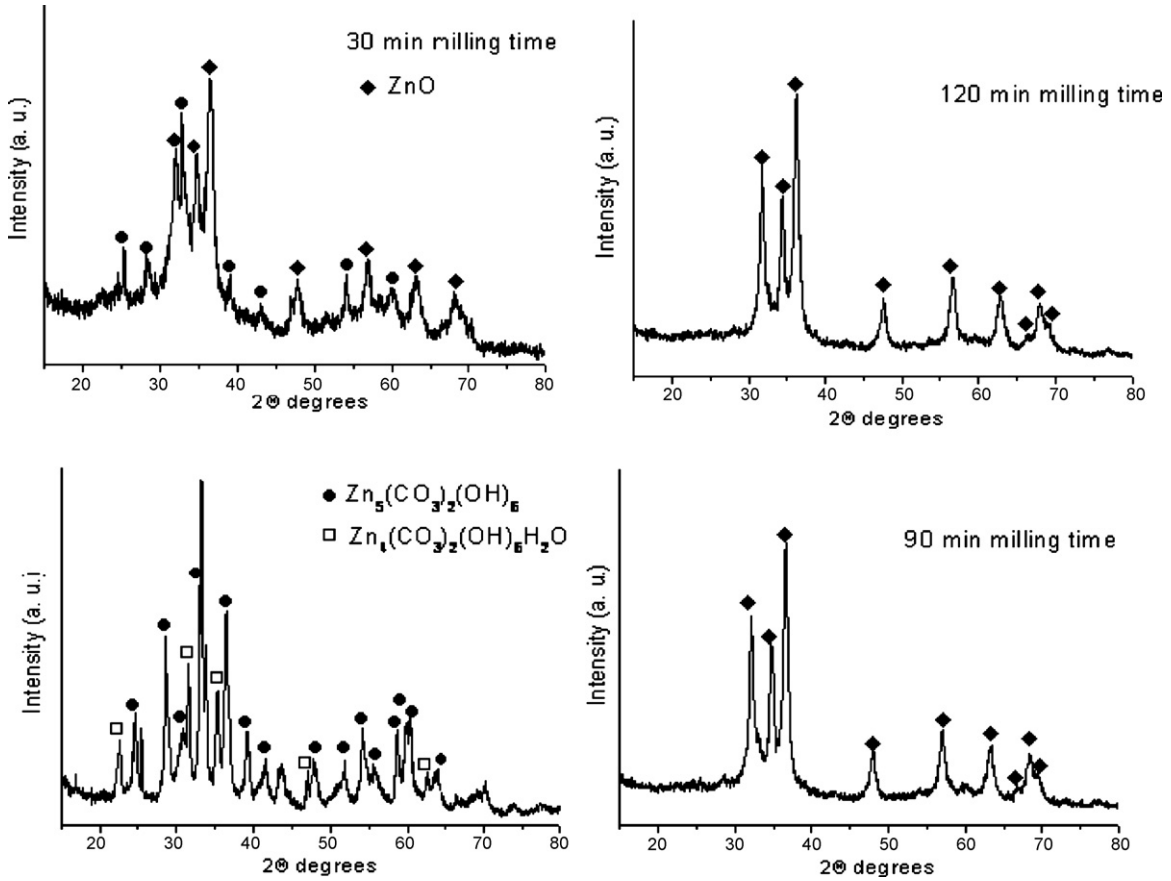

Fig. 2. XRD patterns of the sample B (mechanically treated at 1000 rpm) as a function of milling time.

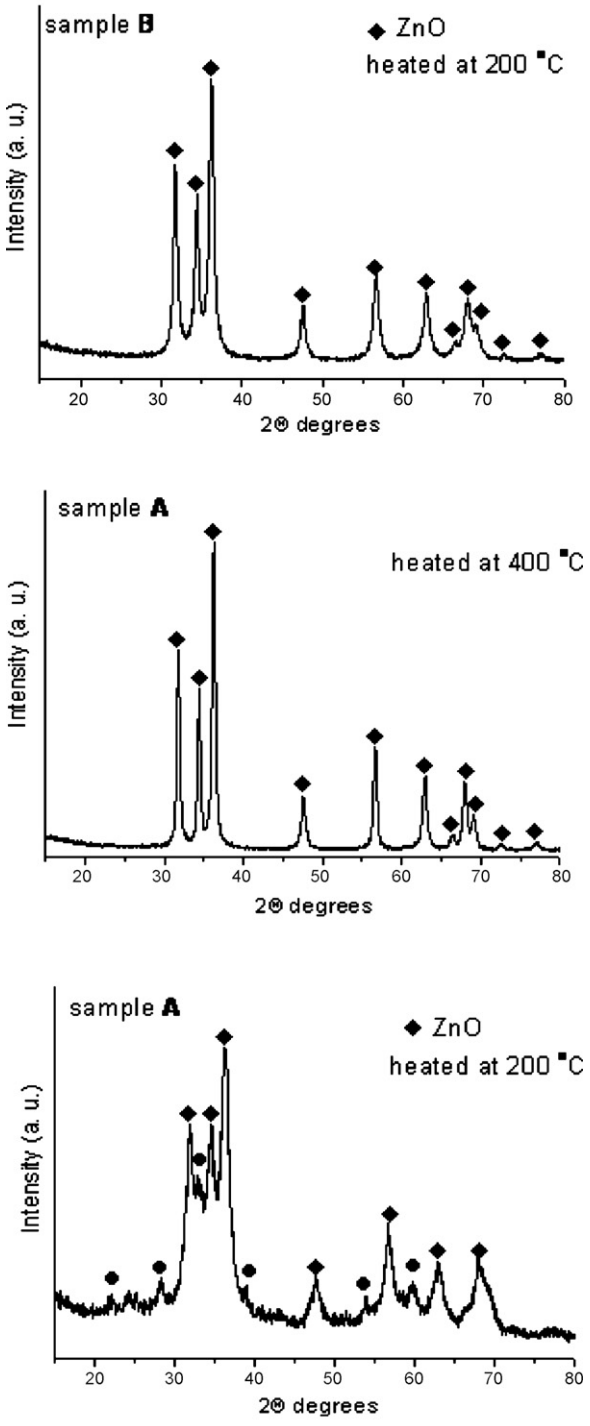

Fig. 3. XRD patterns of the mechanically treated samples (A and B) after heat treatment.

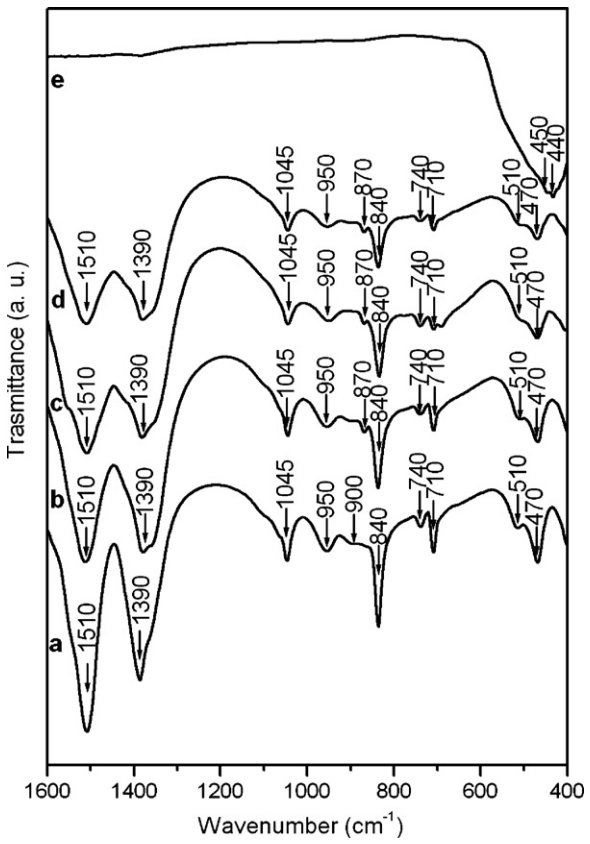

Fig. 4. IR spectra of the sample A (mechanical treatment of 500 rpm): (a) before mechanical treatment; (b) after 60 min milling time; (c) after 120 min milling time; (d) after 600 min milling time; (e) after 600 min milling time and heated at 400 °C.

(i) Sample A, milling speed of 500 rpm, milling time from 60 to 600 min, ball to powder mass ration was 10:1, ball of 5 mm in diameter, heat-treatment at 200 and 400 °C in air for 2 h.

(ii) Sample B, milling speed of 1000 rpm, milling time from 30 to 120 min, ball to powder mass ration was 10:1, ball of 5 mm in diameter, heat-treatment at 200 °C in air for 2 h. The phase and the structural transformations were investigated by X-ray diffraction (XRD) and infrared spectroscopy (IR). Powder XRD patterns were registered with a Bruker D8 Advance diffractometer using Cu-Kα radiation in the 2θ range 15–80°. The "PowderCell" version 2.4 program was used to estimate the average crystallite size of the ZnO powders from the full-width half-maximum of the diffraction peaks. The integral width and the instrumental broadening of the all diffraction peaks were taking into account [36]. "Perfect" Al_2O_3 powder was used as a reference to determine the instrumental resolution function of the diffractometer. The microstrains broadening was not taken into account and that yield to a higher estimate of the particle size. The ICP (optical emission spectrometer inductively coupled plasma) analysis showed that the sample mechanically treated at 1000 rpm for 90 min milling time contains 41,884 mg/l (0.08 at%) of Fe metal as contaminants. Infrared spectra were registered in the range 1600–400 cm^{-1} on a Nicolet-320 FTIR spectrometer using the KBr pellet technique. The morphology of the obtained ZnO powders was analyzed by scanning electron microscopy (JEOL-JSM 6390). The specific surface area of the samples was measured using a modified BET method. The optical properties were measured at room temperature using Evolution 300 UV–VIS Spectrophotometer in the range 200–1000 nm wavelength. The photocatalytic activities of the obtained ZnO powders were evaluated by degradation of a model aqueous solution of Malachite Green (MG) upon UV-light irradiation. The UV illumination was carried out by UV-lamp (Sulvania BLB, 18 W, λ ~315–400 nm). A Malachite Green (MG) solution (150 mL, 5 ppm) containing 0.1 g of as-prepared powder was placed in a glass beaker. Before the light was turned on, the solution was first ultrasonicated for 10 min and then stirred for 10 min to ensure equilibrium between the powders and the solution. Volumes of 3 ml solution were taken at given time intervals and separated through centrifugation (5000 rpm, 5 min). Then the concentration of MG in the solution was investigated with a Jenway 6400 spectrophotometer.

3. Results and discussion

Fig. 1 shows the results from the XRD study of sample A (mechanical treatment at 500 rpm). The process of amorphization started at 60 min and finished after 600 min milling time. As obtained X-ray amorphous sample was heat-treated at 200 °C and ZnO (JCPDS-36-1451) crystals and $Zn_5(CO_3)_2(OH)_6$ were formed. The full synthesis of ZnO was achieved after heat treatment at 400 °C for 2 h and average crystallite size was 20 nm (Fig. 3). The increase in milling speed to 1000 rpm (sample B) led to the direct synthesis of ZnO that began at 30 min and accomplished after 90 min milling time. The average crystallite size of the obtained

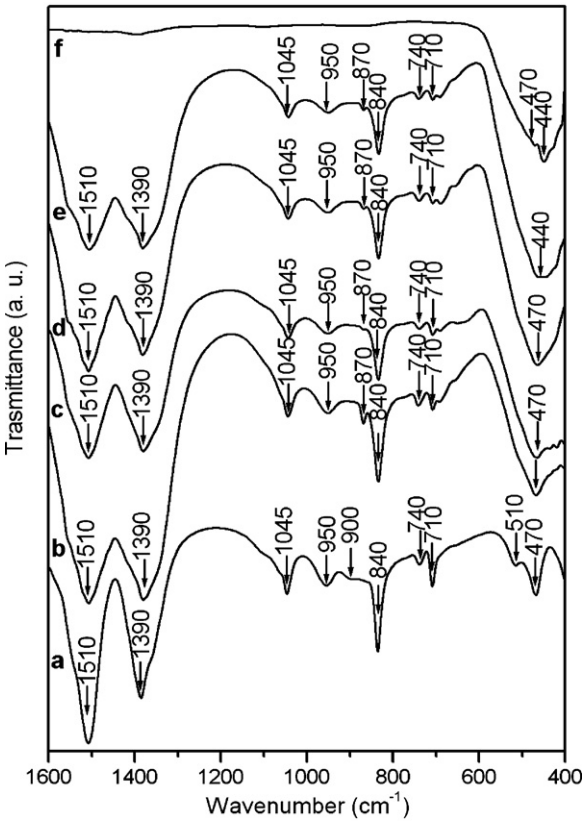

Fig. 5. IR spectra of the sample B (mechanical treatment of 1000 rpm): (a) before mechanical treatment; (b) after 30 min milling time; (c) after 90 min milling time; (d) after 120 min milling time; (e) after 120 min milling time and heated at 200 °C.

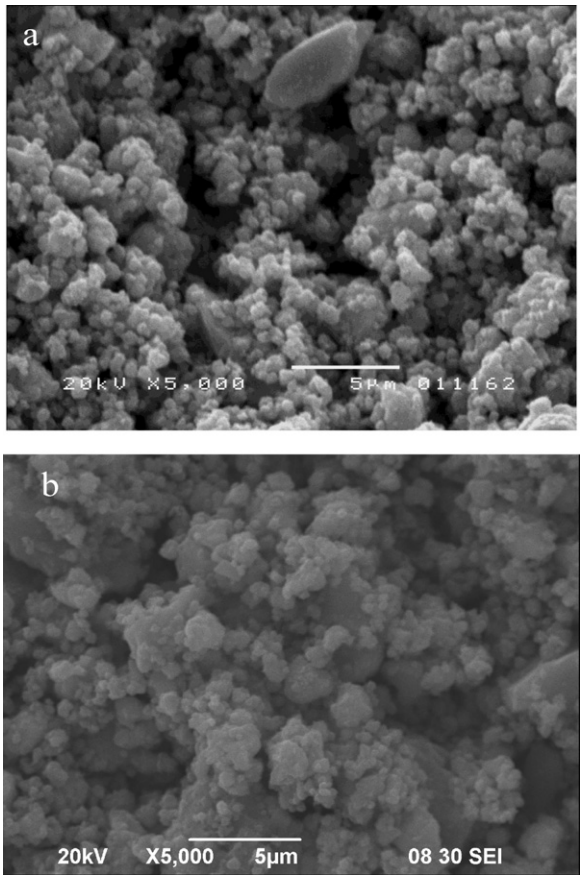

Fig. 6. (a) SEM image of sample A (mechanical treatment of 500 rpm and heated at 400 °C).
(b) SEM image of sample B (mechanical treatment of 1000 rpm and heated at 200 °C).

ZnO powders was 8 nm (Fig. 2). New phase transformation and significant size changes of ZnO particles after additional mechanical treatment up to 120 min were not observed. Heat-treatment at 200 °C led to small increase in crystalline size up to 13 nm (Fig. 3). According to literature data the thermal decomposition of zinc carbonate hydroxide was carried out in the temperature range from 250 to 600 °C [22–25]. We showed that this process can be realized by high milling speed (1000 rpm) without additional thermal treatment. On the other hand calcination at lower temperature (400 °C) led X-ray amorphous sample (obtained at 500 rpm milling speed) to be transformed in pure ZnO.

The additional information for the phase and structural transformations was obtained by IR spectroscopy (Figs. 4 and 5). According to K. Nakamoto, the free ion, CO_3^{2-} exhibits four normal vibration modes: a symmetric stretching vibration (ν_1); an out-of-plane vibration (ν_2); a doubly degenerate asymmetric stretching (ν_3) and doubly degenerate bending modes (ν_4) [37]. The detail investigations of the vibration spectra of hydrozincite ($Zn_5(OH)_6(CO_3)_2$) were carried out by Musić et al. [23], Stoilova et al. [38], and Frost et al. [39]. All characteristic bands of CO_3^{2-} groups we observed in IR spectra of the samples mechanochemcally treated at room temperature (Fig. 4 b–d and Fig. 5 b–e). The presence of these bands in the IR spectrum (Fig. 4 d) of X-ray amorphous sample indicates that an amorphization of zinc carbonate hydroxide took place [23,37–39]. On the other hand the presence of vibration bands characteristic of CO_3^{2-} groups along with the dominant band at 470 cm^{-1} (characteristic for the vibration of ZnO [7,14,23,37–40]) in the IR spectrum of sample B show that transformation of zinc carbonate hydroxide to ZnO is not accomplished at these mechanochemical conditions. According to XRD data of same sample pure ZnO was detected only (Fig. 2). IR spectra of both samples (A and B) after heat treatment indicated presence of ZnO only which is in agreement with XRD data (Fig. 3). The performed analysis manifest that IR spectroscopy is more sensitive and appropriate technique for evolution of some details during phase transformation and decomposition of the materials. Following the IR analysis about ZnO made by Andres-Verges and Martinez Gallego [40] the some conclusions could be drawn for the morphology of ZnO crystals. The presence of an intensive band at 470 cm^{-1} in the IR spectra of samples A and B is typical for the spherical shape of the separate crystals.

Fig. 6(a and b) shows the SEM images of ZnO powders obtained after mechanical treatment (500 and 1000 rpm) and heated at 400 and 200 °C, respectively. Separate spherical grains below 50 nm are joined together into bigger agglomerates. The process of agglomeration of the particles is probably due to the sintering effect during heat-treatment. The specific surface area of obtained ZnO powders after heat-treatment at 200 and 400 °C is 48 and 40 m^2/g, respectively.

Optical transmission spectra of ZnO powders in the UV/vis range are presented in Fig. 7a. The obtained powders are characterized by absorption edge at about 400 nm estimated by the wavelength at which the transmission is 50% of that at the excitonic peak [41,42]. Optical transmission spectra revealed that all mechanochemically treated samples are transparent in the visible region (above 50%) and transparency reached to 80% after heat-treatment (Fig. 7a). In order to calculate the direct band gap of ZnO powder, we have used the Tauc's relationship [43] as follows: $\alpha h\nu = A(h\nu - E_g)^n$ where α is the absorption coefficient, A is a constant, h is Plank's constant, ν is the photon frequency, E_g is the optical band gab and n is 1/2 for

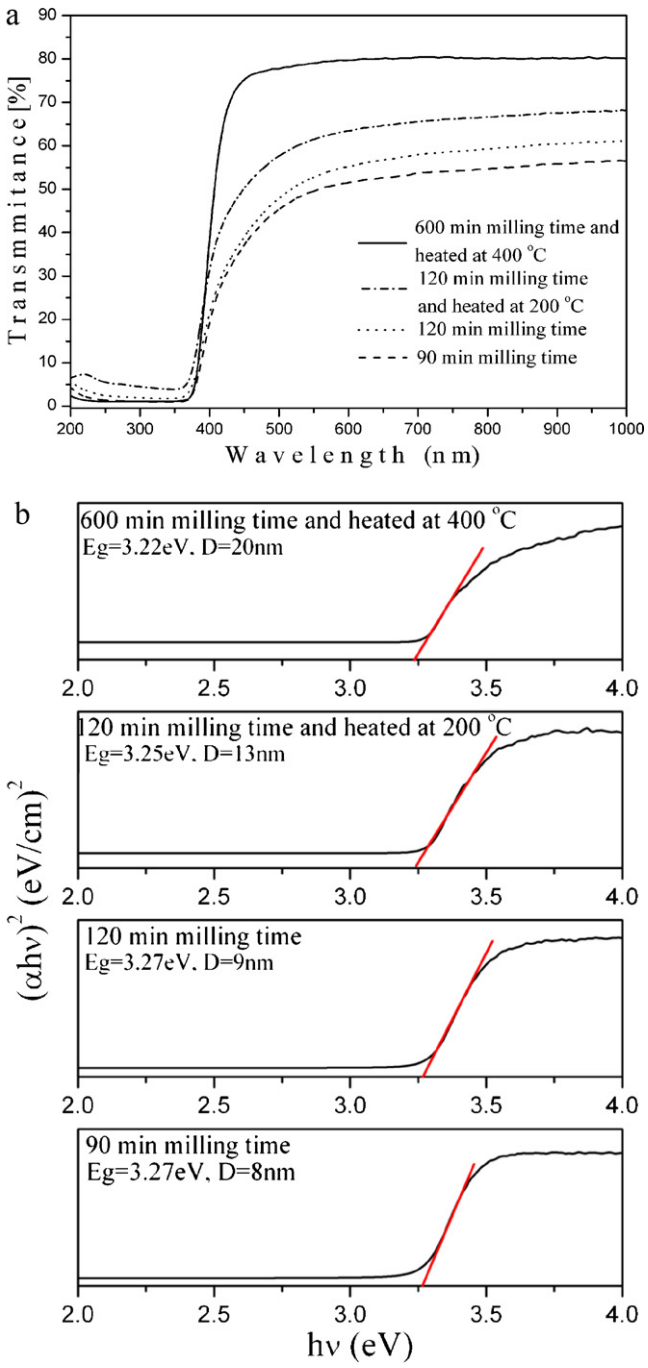

Fig. 7. (a) Optical transmittance spectra and (b) energy band gap of ZnO powders.

direct semiconductor. An extrapolation of the linear region of a plot of $(\alpha h\nu)^2$ on the y-axis versus photon energy $(h\nu)$ on the x-axis gives the value of the optical band gap E_g (Fig. 7b). The calculated band gap was found to decrease from 3.27 to 3.22 eV, with the increase in average crystallite size of ZnO powders. Our results are in good agreement with the data published for ZnO nanoparticles obtained by different synthesis method [14–16,18,29–31,41]

Fig. 8 shows the temporal evolution of the concentration (C/C_o) of MG, where C_o and C represent the initial equilibrium concentration and reaction concentration of MG, respectively. All ZnO powders possess photocatalytic activity under UV-light irradiation. It can be seen that the degradation rate of MG increases with increasing of the temperature and the crystallite size.

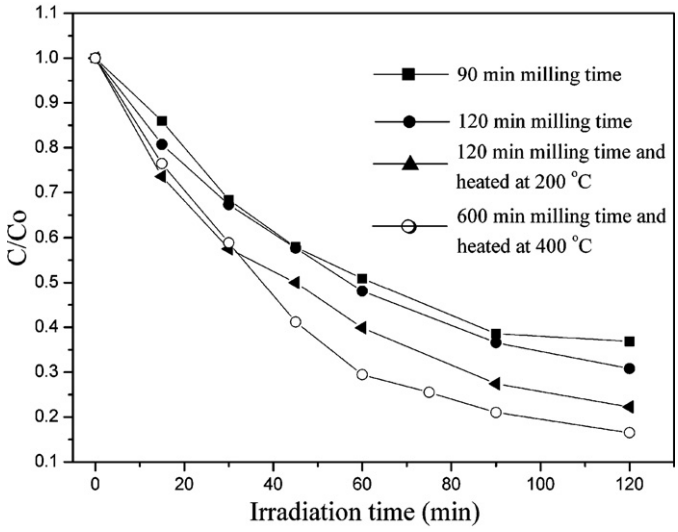

Fig. 8. Decomposition of the MG during UV-light irradiation by obtained ZnO powders.

4. Conclusions

Mechanical treatment of the zinc carbonate hydroxide is an appropriate approach for the preparation of ZnO nanoparticles. We found that the higher milling speed led to direct synthesis of ZnO, while the lower milling speed induced the amorphization of the zinc carbonate hydroxide which was transformed into pure ZnO after heat treatment (400 °C). Optical transmission and photocatalytic activity of ZnO powders increases with increase in average particles size.

Acknowledgments

The study was performed by the financial support of The Ministry of Education and Science of Bulgaria, The National Science Fund of Bulgaria, Contract No TK-X-1702/07 and National Centre for New Materials UNION, Contract No DO-02-82/2008.

References

[1] J.K. Gupta, Application of zinc oxide varistors, J. Am. Ceram. Soc. 73 (1990) 1817–1840.
[2] S. Bernik, G. Branković, S. Rustja, M.Ž. Zunic, M. Podlogar, Z. Branković, Microstructural and compositional aspect of ZnO-based varistor ceramics prepared by direct mixing of the constituent phases and high-energy milling, Ceram. Int. 34 (2008) 1495–1502.
[3] J.H. Lim, C.K. Kang, K.K. Kim, I.K. Park, D.K. Hwang, S.J. Park, UV electroluminescence emission from ZnO light-emitting diodes grown by high temperature radiofrequency sputtering, Adv. Mater. 18 (2006) 2720–2724.
[4] A. Mitra, R.K. Thareja, V. Ganesan, A. Gupta, R.K. Sahoo, V.N. Kulkarni, Synthesis and characterization of ZnO thin films for UV laser, Appl. Surf. Sci. 174 (2001) 232–239.
[5] T. Gao, T.H. Wang, Synthesis and properties of multipod-shaped ZnO nanorods for gas-sensors application, Appl. Phys. A80 (2005) 1451–1454.
[6] Y. Jang, C. Simer, T. Ohm, Comparison of zinc oxide nanoparticles and its nanocrystalline particles on the photocatalytic degradation of methylene blue, Mater. Res. Bull. 41 (2006) 67–77.
[7] C. Hariharan, Photocatalytic degradation of organic contaminants in water by ZnO nanoparticles: revisited, Appl. Catal. A: Gen. 304 (2006) 56–61.
[8] K. Takanezawa, K. Hirota, Q.S. Wei, K. Tajima, K. Hashimoto, Efficient charge collection with ZnO nanorod array in hybrid photovoltaic devices, J. Phys. Chem. C 111 (2007) 7218–7223.
[9] D.P. Norton, Y.W. Heo, M.P. Ivill, K. Ip, S.J. Pearton, M.F. Chisholm, T. Steiner, ZnO: growth doping & processing, Mater. Today 7 (2004) 34–40.
[10] U. Özgür, Y. Alivov, C. Liu, A. Take, M.A. Reshchikov, S. Doğan, V. Avrutin, S. Cho, H. Morkoc, A comprehensive review of ZnO materials and devices, J. Appl. Phys. 98 (2005) 041301–041305.
[11] H. Morkoc, U. Özgür, Zink Oxide, Wiley-VCH, Verlag GmbH&Co, KCaA, 2009.
[12] D. Li, H. Haneda, Morphologies of zinc oxide particles and their effects on photocatalysis, Chemosphere 51 (2003) 129–137.

[13] R. Savu, P. Parra, E. Joanni, B. Jančar, S.A. Eliziario, R. Camargo, P.R. Bueno, J.A. Varela, E. Longo, M.A. Zaghete, The effect of cooling rate during hydrothermal synthesis of ZnO nanorods, J. Cryst. Growth 311 (2009) 4102–4108.
[14] Z. Yang, Q.H. Liu, Controllable synthesis and optical characterizations of ZnO nanostructures by citric acid-assisted annealing process, Physica E 40 (2008) 531–535.
[15] U. Manzoor, M. Islam, L. Tabassam, S.U. Rahman, Quantum confinement effect in ZnO nanoparticles synthesized by coprecipitate method, Physica E 41 (2009) 1669–1672.
[16] P. Uthirakumar, C.H. Hong, Effect of annealing temperature and pH on morphology and optical property of highly dispersible ZnO nanoparticles, Mater. Charact. 60 (2009) 1305–1310.
[17] Y. Gui, C. Xie, A novel simplified method for preparation ZnO nanoneedles via H_2O_2 pre-oxidation, Chem. Phys. 93 (2005) 539–543.
[18] Z. Ji, S. Zhao, C. Wang, K. Liu, ZnO nanoparticles films preparation by oxidation of metallic zinc in H_2O_2 solution and subsequent process, Mater. Sci. Eng. B 117 (2005) 63–66.
[19] S. Hwangbo, Y.J. Lee, K.S. Hwang, Photoluminescence of ZnO layer on commercial glass substrate prepared by sol–gel process, Ceram. Int. 34 (2008) 1237–1239.
[20] Y. Dimitriev, Y. Ivanova, A. Staneva, L. Alexandrov, M. Mancheva, R. Yordanova, C. Dushkin, N. Kaneva, C. Iliev, Synthesis of submicron powders of ZnO and ZnO-M_nO_m (M_nO_m = TiO_2, V_2O_5) by sol–gel methods, J. Univ. Chem. Technol. Metall. 44 (2009) 235–242.
[21] L. Spanhel, M.A. Andersom, Semiconductors culsters in the sol-gel process: quantized aggregation, gelation and crystal growth in concentrated ZnO colloids, J. Am. Chem. Soc. 113 (1991) 2826–2833.
[22] F.A. Sigoli, M.R. Davolos, M. Jafelicci Jr., Morphological evolution of zinc oxide originating from zinc hydroxide carbonate, J. Alloys Compd. 262–263 (1997) 292–295.
[23] S. Musić, S. Popović, M. Maljković, D. Dragcević, Influence of synthesis procedure on the formation and properties of zinc oxide, J. Alloys Compd. 347 (2002) 324–332.
[24] N. Kanari, D. Mishra, I. Gaballah, B. Dupre, Thermal decomposition of zinc carbonate hydroxide, Thermochim. Acta 410 (2004) 93–100.
[25] W. Wu, Q. Jiang, Preparation of nanocrystalline zinc carbonate and zinc oxide via solid-state reaction at room temperature, Mater. Lett. 60 (2006) 2791–2794.
[26] T. Tsuzuki, P.G. McCormick, ZnO nanoparticles synthesized by mechanochemical processing, Scr. Mater. 44 (2001) 1731–1734.
[27] R. Aghababazadeh, B. Mazinani, A. Mirhabibi, M. Tamizifar, ZnO nanoparticles synthesized by mechanochemical processing, J. Phys. 26 (2006) 312–314.
[28] W. Ao, J. Li, H. Yang, X. Zeng, X. Ma, Mechanochemical synthesis of zinc oxide nanocrystalline, Powder Technol. 168 (2006) 148–151.
[29] A. Moballegh, H.R. Shahverdi, R. Aghababazadeh, A. Mirhabibi, ZnO nanoparticles obtained by mechanochemical technique and the optical properties, Surf. Sci. 601 (2007) 2850–2854.
[30] A. Dodd, A. McKinley, M. Saudres, T. Tsuzuki, Effect of particle size on the photocatalytic activity of nanoparticlate zinc oxide, J. Nanopart. Res. 8 (2006) 43–51.
[31] A. Dodd, A. McKinley, T. Tsuzuki, M. Saunders, A comparative evaluation of the photocatalytic and optical properties of nanoparticulate ZnO synthesised by mechanochemical processing, J. Nanopart. Res. 10 (2008) 243–248.
[32] V.V. Boldyrer, Mechanochemistry and mechanical activation of solids, Russ. Chem. Rev. 75 (2006) 203–216.
[33] V.V. Zyryanov, Mechanochemical synthesis of complex oxides, Russ. Chem. Rev. 77 (2008) 105–135.
[34] V. Avvakumov, M. Senna, N. Kosova, Soft Mechanochemical Synthesis: A Basis for New Chemical Technologies, Kluwer Academic Publishers, Boston, 2001.
[35] J.G. Baek, T. Isob, M. Senna, Synthesis of pyrochlore-free $0.9Pb[Mb_{1/3}Nb_{2/3}]O_3$–$0.1PbTiO_3$ ceramics via a soft mechanochemical route, J. Am. Ceram. Soc. 80 (1997) 973–977.
[36] W. Kraus, G. Nolze, PowderCell for Windows, version 2.4, Federal Institute for Materials Research and Testing, Rudower Chanssee 5, 12489, Berlin, Germany, 2000.
[37] K. Nakamoto, Infrared and Raman Spectra of Inorganic and Coordination Compounds, 5th Part A, John Wiley & Sons, Inc., New York, 1997.
[38] D. Stoilova, V. Koleva, V. Vassileva, Infrared study of some synthetic phases of malachite ($Cu_2(OH)_2CO_3$)–hydrozincite ($Zn_5(OH)_6(CO_3)_2$) series, Spectrochim. Acta A 58 (2002) 2051–2059.
[39] R.L. Frost, W.N. Martenes, D.L. Wain, M.C. Hales, Infrared and infrared emission spectroscopy of the zinc carbonate mineral smithsonite, Spectrochim. Acta A 70 (2008) 1120–1126.
[40] M. Andres-Verges, M. Martinez Gallego, Spherical and rod-like zinc oxide microcrystals: morphological characterization and microstructural evolution with temperature, J. Mater. Sci. 27 (1992) 3756–3762.
[41] E.A. Meulenkamp, Synthesis and growth of ZnO nanoparticles, J. Phys. Chem. B 10 (1998) 5566–5572.
[42] W. Vogel, Glass Chemistry, Springer-Verlag, 1994, p. 224.
[43] J. Tauc (Ed.), Amorphous and Liquid Semiconductor, Plenium Press, New York, 1974, p. 159.